

INVERSE SCATTERING OF A BURIED IMPERFECT CONDUCTOR

Wei-Ting Chen and Chien-Ching Chiu

Electrical Engineering Department, Tamkang University

Tamsui, Taiwan, R.O.C.

Email: chiu@ee.tku.edu.tw

Abstract -The problem of determining the shape of an imperfectly conducting cylinder buried in a half-space by the genetic algorithm is investigated. Assume that a conducting cylinder of unknown shape and conductivity is buried in one half-space and scatters the field incident from another half-space where the scattered field is measured. Based on the boundary condition and the measured scattered field, a set of nonlinear integral equations is derived and the imaging problem is reformulated into an optimization problem.

I. Introduction

The image problem of conducting objects has been a subject of considerable importance in noninvasive measurement, medical imaging, and biological application. In the past 20 years, many rigorous methods have been developed to solve the exact equation. However, inverse problem of this type are difficult to solve because they are ill-posed and nonlinear. As a result, many inverse problems are reformulated as optimization problems. General speaking, two main kinds of approaches have been developed. The first is based on gradient search approach such as the Newton-Kantorovitch method [1], the Levenberg-Marguart algorithm [2] and the successive-overrelaxation method [3]. This method is highly dependent on the initial guess and tends to get trapped in a local extreme. In contrast, the second approach is based on the genetic algorithm [4]. It usually converges to the global extreme of the problem, no matter what the initial estimate is. A few papers [4]-[5] use the genetic algorithm to reconstruct the shape of a conductor. However, to our knowledge, there is still no numerical results by the genetic algorithm for the buried imperfectly conducting scatterers. In this paper, we present a method based on the genetic algorithm to recover the shape of a buried imperfectly conducting cylinder.

II. Theoretical Formulation

Let us consider a imperfectly conducting cylinder buried in a lossy homogeneous half-space, as shown in Fig 1. Media in regions 1 and 2 are characterized by permittivity and conductivity (ϵ_1, σ_1) and (ϵ_2, σ_2) respectively. The metallic cylinder with cross section described in polar coordinates in xy plane by the equation $\rho = F(\theta)$ is illuminated by transverse magnetic (TM) waves. We assume that time dependence of

the field is harmonic with the factor $\exp(j\omega t)$. Let E^{inc} denote the incident field from region 1 with incident angle ϕ_1 . For a TM incident wave, the scattered field can be expressed as

$$E_s(x, y) = -\int_0^{2\pi} G(x, y; F(\theta'), \theta') J(\theta') d\theta' \quad (1)$$

where $J(\theta) = -j\omega\mu_0 \sqrt{F^2(\theta) + F'^2(\theta)} J_s(\theta)$

$$G(x, y, x', y') = \begin{cases} G_1(x, y, x', y') & , y \leq -a \\ G_2(x, y, x', y') = G_f(x, y, x', y') + G_b(x, y, x', y') & , y > -a \end{cases} \quad (2)$$

Here $J_s(\theta)$ is the induced surface current density which is proportional to the normal derivative of electric field on the conductor surface. $G(x, y, x', y')$ is the Green's function which can be obtained by Fourier transform. The boundary condition at the surface of the scatterer given by [6] then yield an integral equation for $J(\theta)$:

$$E_s(F(\theta), \theta) = \int_0^{2\pi} G_2(F(\theta), \theta; F(\theta'), \theta') J(\theta') d\theta' + j \sqrt{\frac{j}{\omega\mu_0\sigma}} \frac{J(\theta)}{\sqrt{F^2(\theta) + F'^2(\theta)}} \quad (4)$$

For the direct scattering problem, the scattered field, E_s , is calculated by assuming that the shape and the conductivity of the object are known. This can be achieved by first solving J in (4) and calculating E_s in (2). The shape $F(\theta)$ function can be expanded as:

$$F(\theta) = \sum_{n=0}^{N/2} B_n \cos(n\theta) + \sum_{n=1}^{N/2} C_n \sin(n\theta) \quad (5)$$

where B_n and C_n are real coefficient to be determined, and $N+1$ is the number of unknowns for shape function. The genetic algorithm is used to minimize the cost function:

$$CF = \left\{ \frac{1}{M} \sum_{m=1}^M |E_s^{mea}(r_m) - E_s^{cal}(r_m)|^2 + \alpha |F'(\theta)|^2 \right\}^{1/2} \quad (6)$$

where M , is the total number of measured points. $E_s^{mea}(\bar{r})$ and $E_s^{cal}(\bar{r})$ are the measured scattered field and the calculated scattered field respectively. The minimization of $\alpha |F'(\theta)|^2$ can be interpreted as the smoothness requirement for the boundary of $F(\theta)$. The basic GA for which a flowchart is shown in Fig. 2.

III. Numerical Results

Let us consider an imperfectly conducting cylinder buried in a half-space ($\sigma_1 = \sigma_2 = 0$). The permittivity in region 1 and region 2 is characterized by $\epsilon_1 = \epsilon_0$ and $\epsilon_2 = 2.55\epsilon_0$ respectively. The frequency of the incident wave is chosen to be 3 GHz. The object is buried at a depth 0.1 m. To reconstruct the shape of the object, the object is

illuminated by incident waves from three different directions and 20 measurement points at equal spacing are used along the interface $y = -a$ for each incident angle. In the example, the shape function is chosen to be $F(\theta) = 0.12 + 0.048 \cos 2\theta$ m with material $\sigma = 3.54 \times 10^7$ s/m. The reconstructed shape function for the best population member is plotted in Fig. 3(a) with the error shown in Fig. 3(b), where DR and DSIG are called shape function and conductivity discrepancies respectively. From Fig. 3, it is clear that the reconstruction of the shape function and conductivity is quite good. The quantity DISG is 2×10^{-2} in the final generation. In addition, we also see that the reconstruction of conductivity does not change rapidly toward the exact value until DR is small enough. This can be explained by the fact that the shape function makes a stronger contribution to the scattered field than the conductivity does. In other words, the reconstruction of the shape function has a higher priority than the reconstruction of the conductivity. In the second example, $F(\theta) = 0.02 + 0.004 \sin 2\theta + 0.008 \sin 3\theta$ m with material $\sigma = 5.8 \times 10^7$ s/m. Good results are obtained in Fig. 4(a) and Fig. 4(b).

IV. Conclusions

We have presented a study of applying the genetic algorithm to reconstruct the shape and conductivity of a metallic object through knowledge of scattered field. Based on the boundary condition and measured scattered field, we have derived a set of nonlinear integral equations and reformulated the imaging problem into an optimization problem. By using the genetic algorithm, the shape and conductivity of the object can be reconstructed from the scattered fields. Numerical results also illustrate that the conductivity is more sensitive to noise than the shape function is.

REFERENCES

- [1] A. Roger, "Newton-Kantorovitch algorithm applied to an electromagnetic inverse problem," *IEEE Trans. Antennas Propagat.*, vol. 29, 232-238, 1981.
- [2] D. Colton and P. Monk, "A novel method for solving the inverse scattering problem for time-harmonic acoustic waves in the resonance region II," *SIAM J. Appl. Math.*, vol. 46, pp. 506-523, June 1986.
- [3] R. E. Kleinman and P. M. van den Berg, "Two-dimensional location and shape reconstruction," *Radio Sci.* vol. 29, pp. 1157-1169, July- Aug. 1994.
- [4] C. C. Chiu and P. T. Liu, "Image reconstruction of a perfectly conducting cylinder by the genetic algorithm," *IEE Proc.-Micro. Antennas Propagat.*, vol. 143, pp.249-253, June 1996.
- [5] F. Xiao and H. Yabe, "Microwave imaging of perfectly conducting cylinders from real data by micro genetic algorithm couple with deterministic method", *IEICE Trans. Electron.*, vol. E81-C, pp. 1784-1792, Dec. 1998.
- [6] F. M. Tesche, "On the inclusion of loss in time domain solutions of electromagnetic interaction problems," *IEEE Trans. Electromagn. Compat.*, vol. 32, pp. 1-4, 1990.

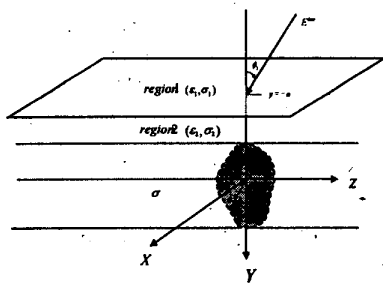


Fig. 1 Geometry of the problem in (x,y) plane

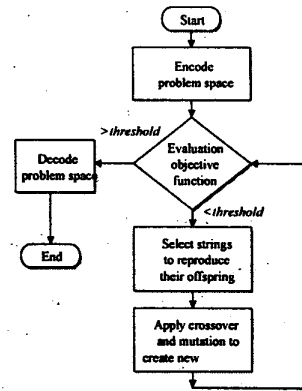


Fig. 2 Flow chart for the genetic algorithm

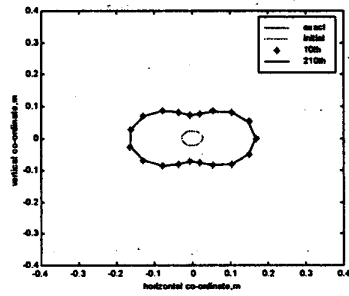


Fig. 3(a) Shape function

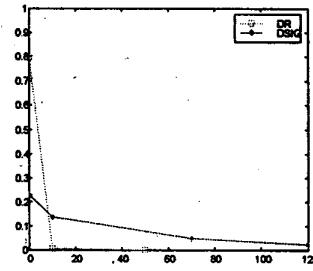


Fig. 3 (b) shape function and conductivity error

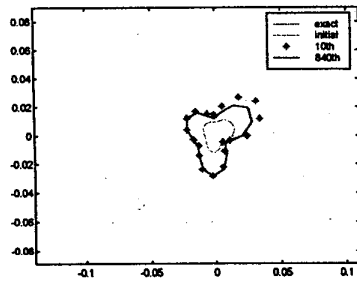


Fig. 4(a) Shape function

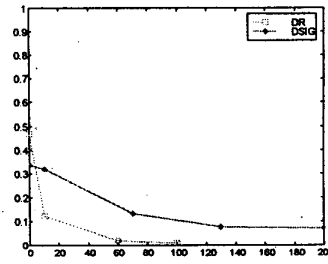


Fig. 4 (b) shape function and conductivity error